# Isotachophoretic Concentration of Biomolecules in Human Biofluids for Low-cost Portable Health Monitoring

by

Steven Doria

A thesis submitted to Johns Hopkins University in conformity with the requirements for the degree of Masters of Science in Engineering

Baltimore, Maryland

May, 2018

# Abstract

Early diagnostics is a key factor in the success of many initiatives; including missions into deep space, rapid response to disease outbreaks, and long-term care of comorbidities of chronic conditions. Unfortunately, in many of the aforementioned scenarios, it is impossible to transport the patient to the hospital, or even a point of care. Thus, there is a clear need for rapid, portable, and inexpensive diagnostic replacements for common tests such as the western blot, and gel electrophoresis. We believe that by applying the concept of isotachophoresis (ITP), or electrophoretic mobility stacking, to microfluidic chips, we can develop a portable, inexpensive, and easy to use replacement for gel electrophoresis and the western blot. We use soft lithographic techniques to fabricate our device. Further, we apply a carbon black membrane between our electrode and main flow channel to improve electric efficiency. In this correspondence, we develop a mathematical model for previous ITP experiments, improve the electrical efficiency of our separation experiment, extend previous experiments on dyes to a relevant biomarker, avidin, and explore changing the analyte media to a relevant biofluid, human serum. Further, we define the critical bubble voltage of our experiments in human serum. We find that we were able to successfully extend our technology to work with avidin and human serum. Further, we were able to reduce the required voltage for separation of dye within our device from 1800 to 200 volts. Finally, we developed a mathematical model that fits our dye experiments. In the future, we will look to change our biofluid to whole blood, and look into using DNA as an analyte. Further, we will look to build upon our existing mathematical model and develop a physical model.

Advisor: Dr. Zachary Gagnon

Reader: Dr. Michael Betenbaugh

# Acknowledgements

Thank you to Dr. Gagnon, my family, and my friends. Without your support, my work would not have been possible.

# Table of Contents

# List of Figures

# Chapter 1

# Introduction

Achieving a manned trip to Mars is a tremendous long-term goal set by numerous public and private organizations. Further, a successful mission would mark the first step in the long journey towards extraterrestrial colonization. A goal that SpaceX hopes to achieve by the 2030s.[1]

The six month journey into deep space presents a myriad of crew health, safety, and performance challenges.[2] Specifically, astronauts are at a higher risk of developing: bone demineralization, cardiovascular dysfunction, and muscular dystrophy.[3] As is true with any affliction, early diagnosis is the first step to a positive patient outcome. Therefore, aforementioned challenges make screening for disease, establishing deviations from personal health norms, and detecting viral and bacterial infection of crewmembers, cabin air, and cabin water vital to the success of any deep space venture.[4]

Protein and DNA separation, namely western blots and gel electrophoresis are two crucial diagnostic tools.[5] Unfortunately, the equipment required to drive these processes is far too bulky to be practical for missions into deep space. Therefore, the long-term goal of this project is to develop a lightweight, and compact diagnostic device capable of simultaneously separating proteins and DNA. Furthermore, our final device will be inexpensive, rapid easy to use, and require minimal sample volume.

We believe a microfluidic approach is the optimal solution to the problem of long-term space-efficient crew diagnostics due to the fact that microfluidic devices tend to achieve relatively high degrees of cost, weight, space, and time efficiency, when compared to their macro counterparts.[6]

Our chip utilizes a physical phenomenon known as isotachophoresis (ITP). ITP simultaneously focuses, and separates analytes based on their electrophoretic mobility. ITP is achieved by flowing the analyte(s) between a leading electrolyte (LE), which has a higher electrophoretic mobility than all analytes, and a tailing electrolyte (TE), which has a lower electrophoretic mobility than all analytes, and applying an electric field across the device. ITP within batch systems is a widely researched.[7] Further, ITP has been applied to continuous systems in a process known as free flow isotachophoresis (FFITP) in select cases. Some of these cases include the separation of analytes from whole blood, specifically high-electrophoretic mobility protein separations, and the analysis of pathogenic bacteria.[8,9,10,11,12] We believe that ITP within a microfluidic device can be an effective replacement for western blots and gel electrophoresis.

Unfortunately, FFITP has many roadblocks preventing its use within more generalized systems, such as our proposed full western blot and gel electrophoresis system. These roadblocks include: Joule heating, bubble generation due to the electrolysis of water, and unwanted electro-osmotic flow.[13] The major problems with generalized ITP within FFITP are caused by the required voltage to resolve proteins and DNA strands with relatively low electrophoretic mobilitys. In order to resolve these proteins, the applied voltage must be increased, which increases the current within the electrolytes, causing the aforementioned roadblocks. Furthermore, the required voltage to achieve these separations would be in the thousands. Equipment capable of driving such a voltage would not meet our weight, space, and cost specifications.

We circumvent the high required voltage by doping the PDMS between the electrodes and the main flow channel with carbon black, reducing the overall electrical resistance between

the two electrodes. The lowered voltage reduces Joule heating, and overall current within the electrolytes. The reduced current, in turn suppresses bubble generation. Further, we utilize HPMC to suppress electro-osmotic flow.[13]

In the past we have applied this technology to dyes in order to show that FFITP is possible within a continuous process.[13] In this correspondence, we expand our technology to relevant biomarkers, namely avidin, while simultaneously adding a mathematical model to our results with dyes. Finally, we bring our idealized model closer to practicality by changing the media to human serum.

Finally, it should be noted that this technology has uses outside of diagnostics within deep space exploration. In fact, this technology is a valuable tool in any scenario where portable, and inexpensive diagnostics is deemed desirable. More specifically, we believe that this technology can provide diagnostic value in crisis situations in under-developed countries such as the recent Zika outbreak. We envision our technology being useful after biological markers have been determined as a quick on-site diagnostic tool. Further, due to the "easy-to-use" nature of our technology, we believe that FFITP can be applied to at home screening for patients who are at high risk for comorbidities with diagnosed conditions. For example, a patient who is diagnosed with diabetes is at a high risk for comorbidities such as fatty liver disease, and cancer. In serious cases, patients could perform monthly at home self-screens, potentially providing the early diagnoses doctors need to save lives.

# Chapter 2

# Background

## 2.1 ITP Background

ITP stacks analytes by their electrophoretic mobility. More specifically, the analyte with the highest electrophoretic mobility will be found closest to the electrode opposite the charge of the analytes. Electrophoretic mobility is defined by:

$$\mu = \frac{v_d}{E} \text{ (Equation 1)}$$

Where:

μ is the electrophoretic mobility

$v_d$ is the drift velocity in a uniform electric field

E is the electric field

It should be noted that the drift velocity, and therefore the electrophoretic mobility, of a species is dependent on both the species itself, and the media the species is present in.

Furthermore, for ITP to be successful, the five following conditions must be true[5]:

1. The LE, TE, and all analytes must have the same charge sign.
2. The electrophoretic mobility of all analytes must be higher than the electrophoretic mobility of the tailing electrolyte within the tailing electrolyte.

3. The electrophoretic mobility of all analytes must be higher than the electrophoretic mobility of the tailing electrolyte within the analytes.
4. The electrophoretic mobility of all analytes must be lower than the electrophoretic mobility of the leading electrolyte within the leading electrolyte.
5. The electrophoretic mobility of all analytes must be lower than the electrophoretic mobility of the leading electrolyte within the analytes.

## 2.2 ITP Theory

ITP can be modeled using the basic mass transfer equations. We define the z-axis as the parallel to the direction of flow, we define the y-axis as the direction of an arrow that points from one electrode to the other. This leaves the x-axis as the direction that points up and down the channel. We assume that there is no change within the x-axis.

Basic mass transfer equation:

$$\frac{\partial C}{\partial t} + \nabla \cdot (\vec{v}\, C) = D(\nabla^2 C) - \mu * \vec{E}(\nabla \cdot (\vec{v}\, C)) \text{ (Equation 2)}$$

Where:

v is the velocity

E is the electric field

D is the diffusivity

t is time

μ is the electrophoretic mobility of a species

C is the concentration of a species

Assuming that our system has reached steady state, and we are sufficiently far down the channel such that no change occurs in the z direction, noting that the electric field is only in the y direction, and that the flow is unidirectional in the z direction, the concentration equation yields:

$$\mu * E(y)\frac{\partial C}{\partial y} = D\frac{\partial^2 C}{\partial y^2} \text{ (Equation 3)}$$

Furthermore, the electric field is not a constant. It can be modeled by the following equation:

$$E(y) = \frac{j}{\sigma} - \frac{F}{\sigma}\sum_i z_i D_i \nabla C_i \text{ (Equation 4)}$$

Where:

σ is the conductivity of the electrolyte

i is any chemical species

$z_i$ is the valency of a chemical species

$D_i$ is the diffusivity of a chemical species

$C_i$ is the concentration of a chemical species

j and F are constants

Equations 3 and 4 can be numerically coupled in order to solve for the expected concentration profile.

### 2.3.1 Electrolysis of Water

The electrolysis of water poses a significant practical problem for all FFITP systems due to the high current within the electrolytes and the analyte.

$$H_2O(l) \rightarrow H_2(g) + \frac{1}{2}O_2(g) \text{ (Equation 5)}$$

The problem, as highlighted in the above reaction, occurs due to the rapid insertion of gasses into the microfluidic channel. These gasses form bubbles, which causes the device to perform unpredictably, limiting the overall usefulness of the device.

The electrolysis reaction puts a practical ceiling on the voltage that can be applied to our device. This ceiling is dependent on the current created in the device. Kinetically, electrolysis is linearly dependent on the current.[14] Therefore, by Ohm's law, the maximum allowed voltage scales linearly with the maximum allowed current. Further, the maximum allowed voltage scales with $R^{-1}$. This relationship is quite important when moving from one media to another.

## 2.3.2 Quinhydrone

In order to combat the electrolysis reaction, we flow quinhydrone on the sides of our channels. Quinhydrone is an electron donor/acceptor complex between hydroquinone, and p-benzoquinone. Furthermore, hydroquinone itself can act as an electron acceptor, and therefore function as a suppressor of the electrolysis of water.[15] More specifically, quinhydrone accepts electrons that would be used for the electrolysis of water.

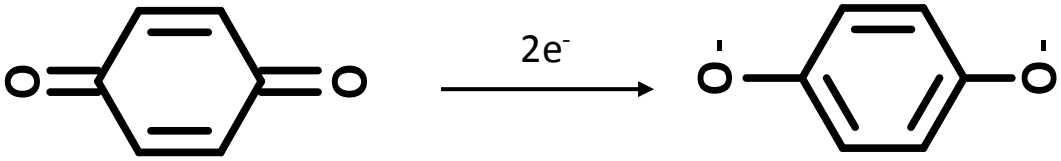


**Figure 1: Quinhydrone as an electron acceptor**

# Chapter 3

# Materials and Methods

## 3.1 Device Geometry

Our device, as shown in figure 2, consisted of one main flow channel with 5 inlet and outlet channels. The main flow channel was 1 cm long 1 mm wide, and 50 microns high. Furthermore, the gap between the main flow channel and the electrodes was 100 microns thick.

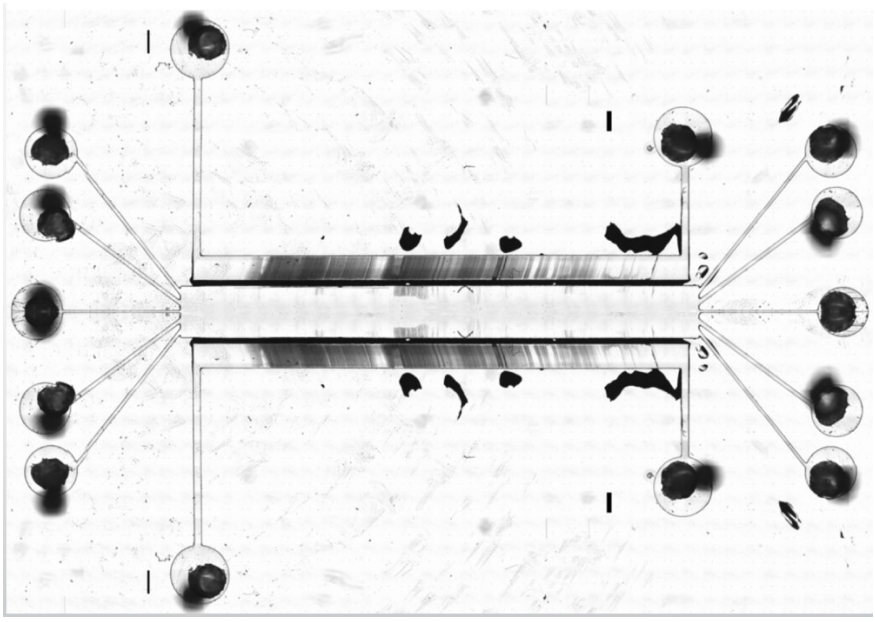

**Figure 2: Bright field image of the device**

## 3.2 Fabrication Overview

We fabricated our microfluidic device using a standard multistage soft lithographic process. This process consisted of developing a negative mold of the device, applying doped

PDMS to the device by hand, then pouring and curing PDMS on top of the negative mold. Finally, we attached the PDMS to a glass coverslip.

### 3.2.1 Negative Mold Fabrication

We fabricated the negative mold by pouring SU-8 3050 (Microchem Corp), a negative photoresist, onto a silica wafer. We then spun the photoresist down to its desired height. In the case of this experiment, this desired height was 50 microns. We then softbaked the wafer at 65°C for two minutes, followed by a subsequent 95°C softbake for three minutes. The primary softbake prevented heat shocking the wafer, which could have caused the negative mold to crack. Next, we aligned a transparent mask and developed the photoresist using UV light. After exposure, we softbaked the wafer for 5 more minutes at 95°C, then bathed the wafer in SU developer. We then went through two more minutes of 65°C softbaking, three more minutes of 95°C softbaking, and finished with a 200°C hardbake for three hours.

### 3.2.2 Carbon Black Application Process

We began by scraping the carbon black (25% wt) doped PDMS onto a pipette tip. We then dragged the tip of the pipette down the negative mold, in between the negatives of the main flow channel and the electrode channel. Next, we took a razor, positioned it such that the razor lined up parallel to the main flow channel, and at a low angle, scraped perpendicularly to the main flow channel. The low angle prevented scratching the negative mold. This cleaned off any excess carbon black from the main flow channel. Note that we applied this process to both sides of the device.

### 3.2.3 PDMS Fabrication

We poured a 1:10 mixture of curing agent to PDMS on top of the silica wafer. This mixture was allowed to cure for 1 hour at 85°C. We then gently removed the PDMS from the mold. We then punched holes into each inlet and outlet using a .75 mm biopsy punch (Ted Pella). After this, we exposed the device, and a glass coverslip to oxygen plasma (Jetlight, Model 42A) and attached the PDMS to the glass coverslip. The PDMS and coverslip were allowed to cure overnight

### 3.2.4 Gallium Electrode

The electrode in our device was made of gallium. We fabricated the electrode by melting solid gallium on a hot plate at 40°C. Note that we placed the device on the same hot plate as the gallium, in order to prevent heat shocking the device when we input the gallium into the electrode channel. We then transported the liquefied gallium from the hot plate, into the electrode channel using a syringe. Before the gallium solidified, we placed metal posts in the inlet channels to create a future location to connect the power source to our device. After the posts are input, the gallium was allowed to cool.

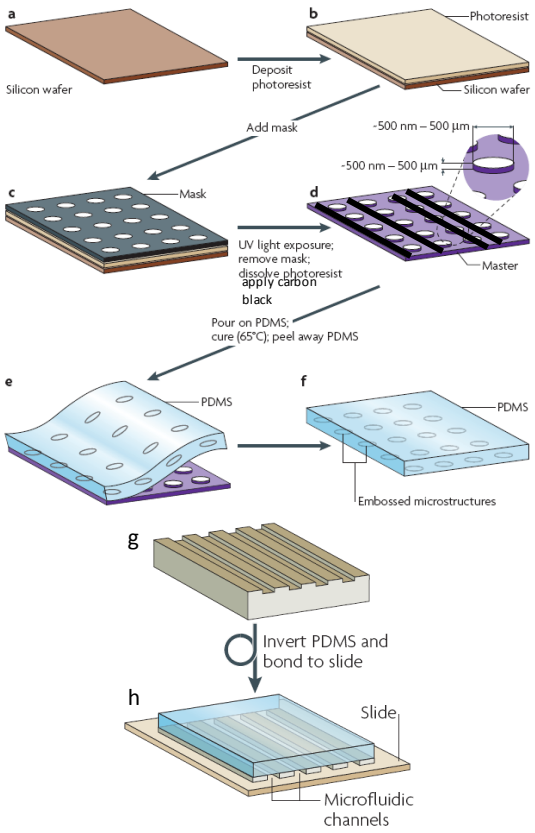


**Figure 3: Fabrication process overview[16]**

## 3.3 Chemicals and Reagents

All chemicals used in this paper were purchased from Sigma-Aldrich unless otherwise stated.

### 3.3.1 Crosslinked PDMS

We made the crosslinked PDMS by adding a 1:10 solution of curing agent and PDMS to a mixing cup. We then mixed the solution in a Thinky ARM 310.

### 3.3.2 Carbon Black Doped PDMS

We make the carbon black doped PDMS by taking the same solution used to make the crosslinked PDMS. We then added carbon black such that the carbon black made up 25% of the total weight of the mixture. Finally, we mixed the mixture in a Thinky ARM 310.

### 3.3.3 Tailing Electrolyte

Using a pipette, we mixed a sample of 10 mM 4-(2-hydroxyethyl)-1-piperazineethanesulfonic acid (HEPES), 20 mM Bis-Tris, .1% HPMC, and 1% Tween 20 by volume. In separation experiments, we prepared stock solutions of 1 mg/mL rhodamine B and 1 mg/mL fluorescein in advance, and diluted by a factor of ten within the tailing electrolyte. In concentration experiments, no analyte was included within the tailing electrolyte.

### 3.3.4 Leading Electrolyte

Using a pipette, we mixed a sample of 10 mM HCl, 20 mM Bis-Tris, .1% HPMC and 1% Tween 20.

### 3.3.5 Quinhydrone

We made the quinhydrone solution by mixing a solution such that 1 mg/mL of hydroquinone and 1 mg/mL of p-benzoquinone was present, and allowing such a solution to naturally form quinhydrone.

### 3.3.6 Human Serum

Our human serum was supplied from pooled donors, and stored in a freezer. Upon unfreezing, we aliquotted the serum into 4 mL samples. Each sample was, at most, unfrozen two times, and refrozen one time within our care.

### 3.3.7 Concentration Analyte

Concentration analytes were prepared by mixing 3900 mL of DI water with 100 mL of analyte. Our analyte stock solutions were 2.5 μM Avidin-FITC, and 1 mg/mL fluorescein.

## 3.4 Flow Control

We connected pressurized house gas to an elveflow control system. The pressurized gas was applied to a sample tube containing reagents, which flowed through a flowmeter and into the chip. The flowmeter fed back a measured flow rate into the elveflow system, creating a feedback control system.

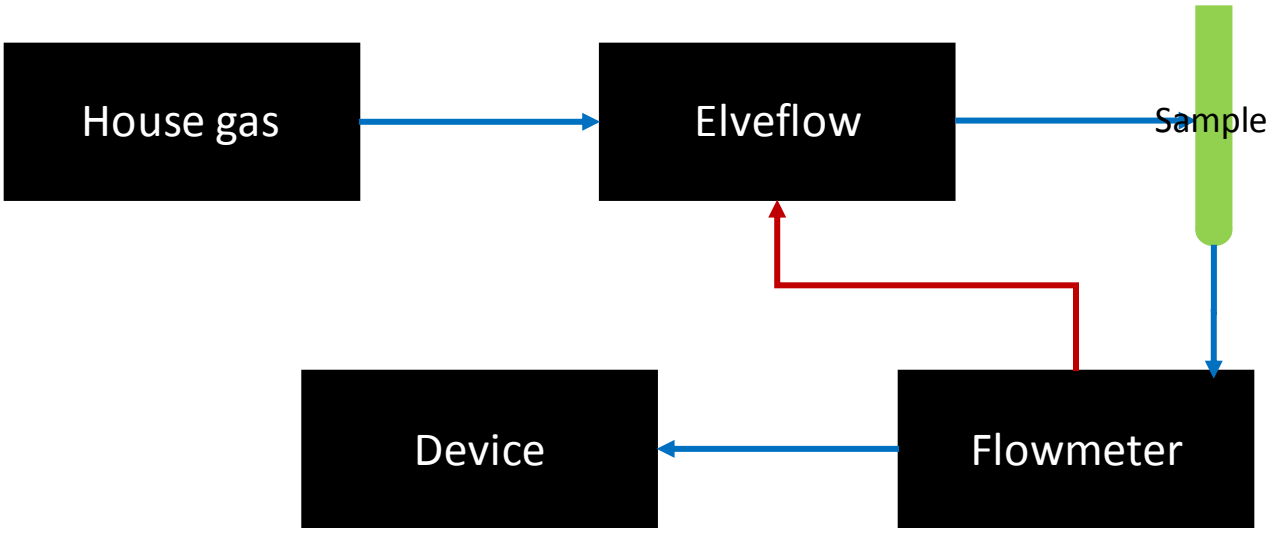


**Figure 4: Flow control diagram**

### 3.5.1 Concentration Experiments

In concentration experiments, we flowed quinhydrone through channels 1 and 5. We simultaneously flowed the LE through channel 2 and the TE through channel 4. Furthermore, we flowed the analyte of interest through channel 3. We varied the flow rate of the analyte from 2 µL/min to 50 µL/min. We flowed both the TE and the LE at the same flowrate as the analyte, whereas the quinhydrone flow was driven at half the flowrate of the analyte. Practically speaking, so long as the width of the quinhydrone profile within the channel is sufficiently large to block bubble formation, the quinhydrone flow rate can be altered as desired, in order to determine what outlet the analyte ends up in, however we keep the quinhydrone flow rate consistent throughout our experiments. We then applied an electric field across the main flow channel, perpendicular to flow, inducing analyte focusing. Voltages from 0 to 200 V were applied across the 1.2 mm gap between electrodes. The electric field was applied such that the analyte was attracted towards the electrode closest to the LE. This is dependent only on the sign

of the charge of the analyte. Further, it should be noted that the LE, TE, and analyte must have the same sign of charge. Flow profiles of fluorescently tagged analytes were imaged using a fluorescent microscope.

### 3.5.2 Concentration of Avidin in Human Serum

Due to the high conductivity of the human serum, suppressing bubble formation became a priority. As a result, the flowrate of the quinhydrone had to be three times higher than the flowrate of the analyte. Specifically, we set the flowrate of the LE, TE, and analyte to 5 uL/min, and the flowrate of the quinhydrone to 15 uL/min.

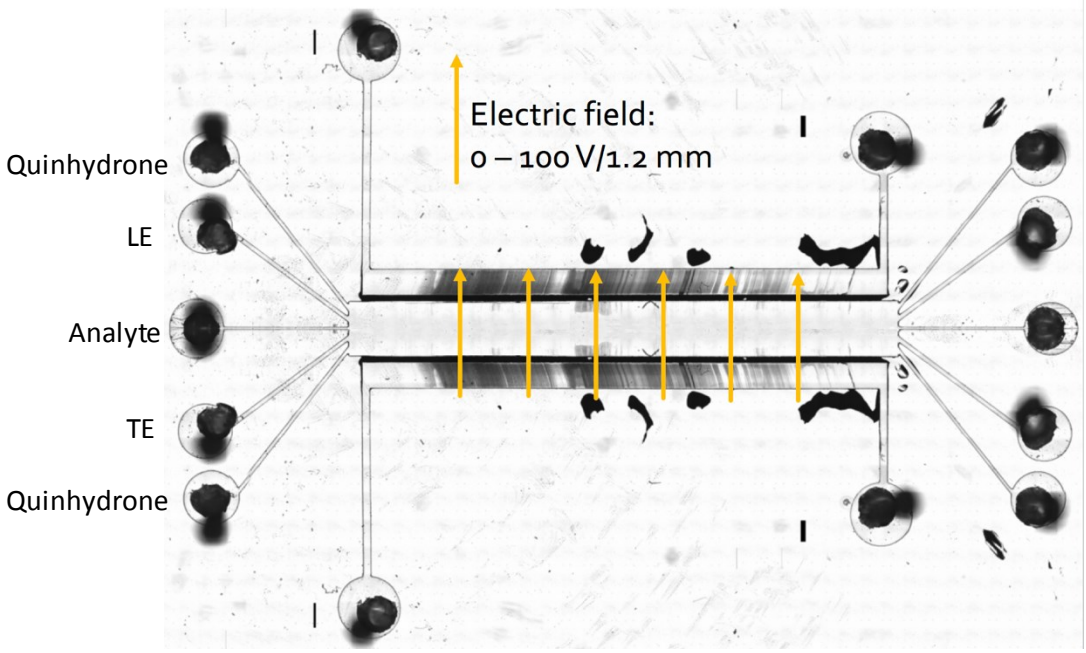


**Figure 5: Concentration experiment setup**

### 3.5.3 Critical Bubble Voltage

The voltage at which bubbles begin to form in the human serum experiment is a major physical constraint of the device due to the fact that bubbles create an unpredictable disruption to fluid flow. Therefore we investigated the critical bubble voltage.

Originally, we attempted to increase the concentration of the quinhydrone, however increasing the concentration by 10 times did nothing to change the critical bubble voltage. We did determine, however, that the critical bubble voltage can be affected by the flowrate of the quinhydrone.

We set the flowrate of the LE, TE, and analyte mixed with human serum to 5 μL/min. We then varied the flowrate of both quinhydrone inlets from 2 to 35 μL/min. At each flowrate, we increased the voltage by 5 until bubbles began to form.

### 3.5.4 Separation Experiments

We conducted separation experiments by flowing quinhydrone through channels 1 and 5. We simultaneously flow LE through channel 2, and the TE mixed with analytes through channel 4. During separation experiments, we plugged channel 3. We applied the same flow rate ratios. Further, the same voltage ranges were used to induce stacking. The voltage was applied such that the direction of the electric field attracted the analyte towards the electrode closest to the LE.

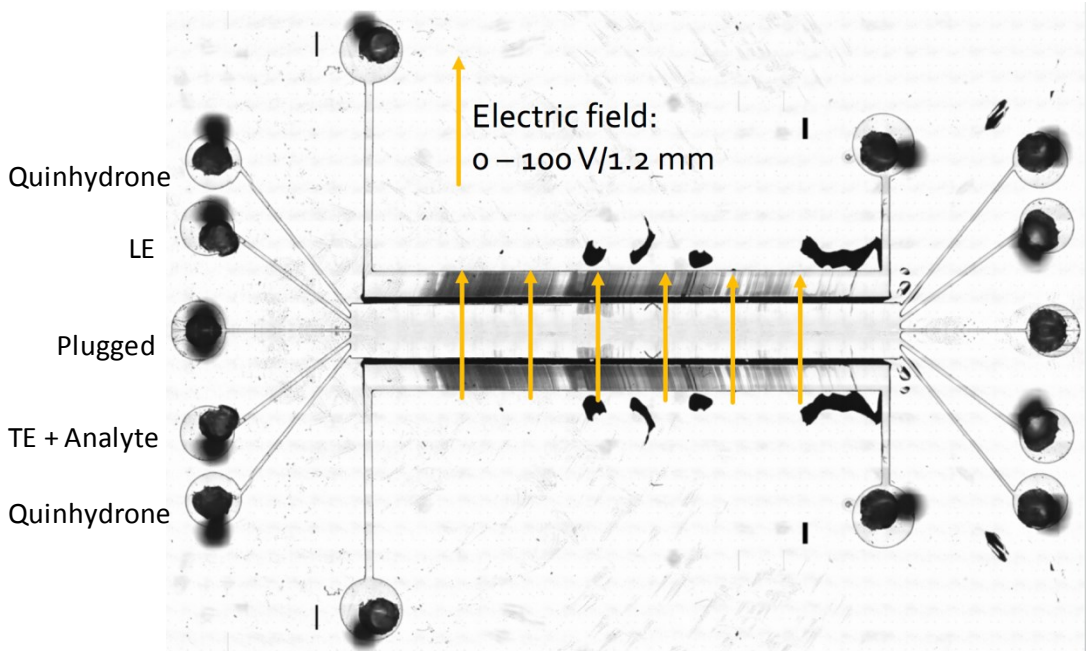


**Figure 6: Separation experiment setup**

# Chapter 4

# Results

## 4.1 Dye Focusing

Dye focusing had already been shown to be possible in our previous correspondences.[13] We have furthered this work to show that dye focusing is possible without pre-mixing of the tailing electrolyte and the analyte.

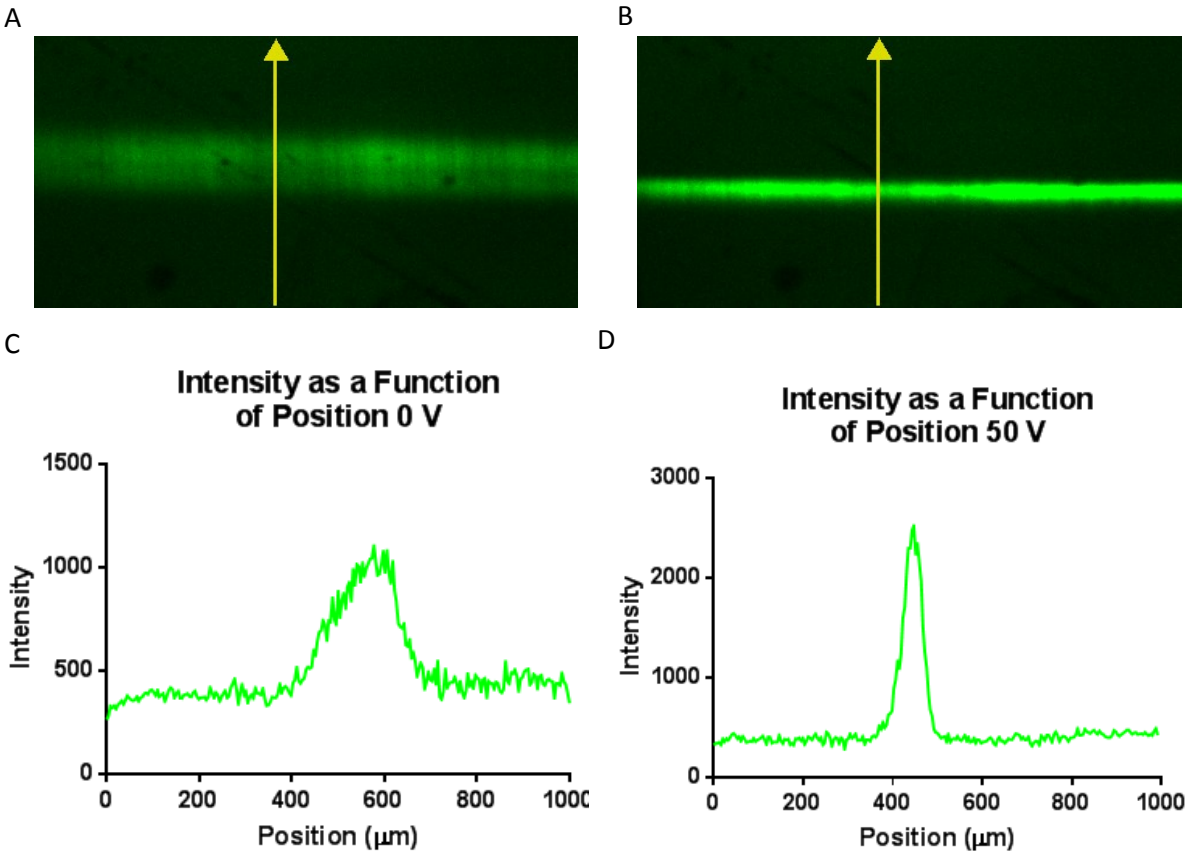


**Figure 7: A fluorescent image of fluorescein focusing experiment without pre-sample mixing. Top left (7A) 2 µL/min, 0V. Top right (7B) 2 µL/min, 50 V. Bottom left (7C) concentration profile of figure 7A. Bottom right (7D) concentration profile of figure 7B.**

Further, we have mathematically modeled the average intensity increase (AII) as a function of both voltage and volume flowrate. In short, we calculate AII by finding the average intensity of the dye at 0V, and then subtract this intensity off of each individual point in the intensity profile. From here, we found the average of all points remaining that are above 0. We modeled this as a decaying exponential function in the following:

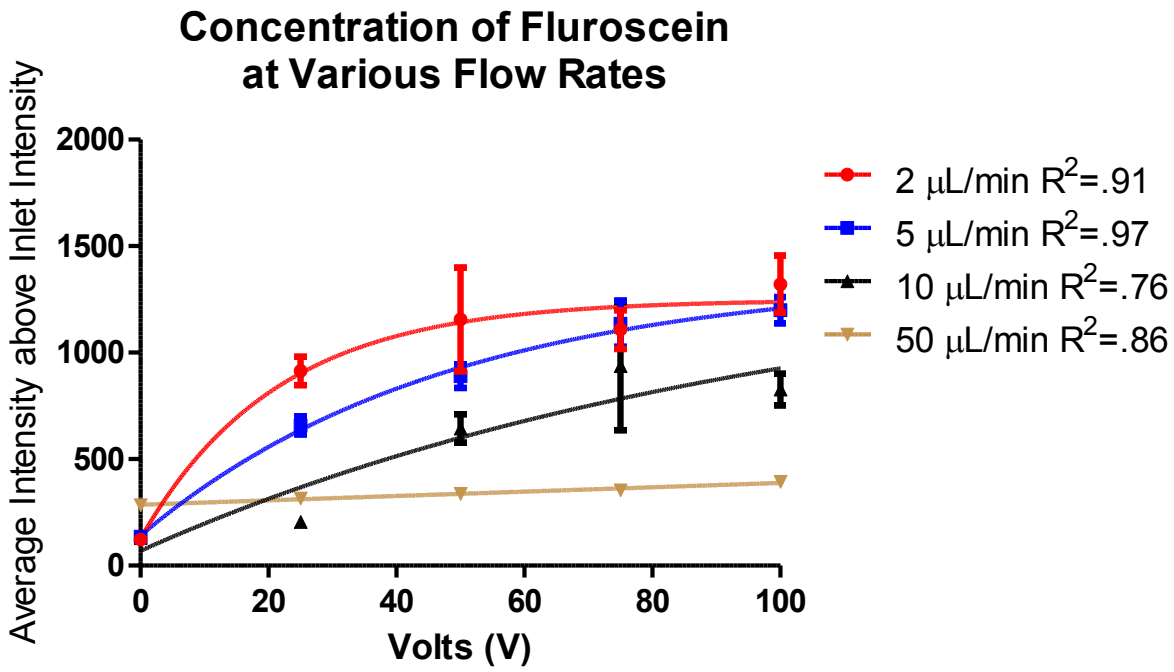


**Figure 8: AII as a function of voltage over 4 separate flowrates. n=5**

The generalized equation for such a model is:

$$AII = A_0 * (1 - \exp(-k * V)) + C \text{ (Equation 6)}$$

Where:

AII is the average intensity increase

$A_0$, C, and k are fitted constants

K is a fitted constant

V is the voltage applied

Further, we found that k is a decaying exponential of the volumetric flowrate:

$$k = k_0 * \exp(-k' * \dot{V})$$ (Equation 7)

Where:

k is the decaying exponential from the AII equation

$k_0$ is an experimentally determined constant, which represents the theoretical k at 0 μL/min

k' is the exponential decay constant of k, and is also experimentally determined

$\dot{V}$ is the volumetric flow rate

We graph k for 4 separate flow rates below:

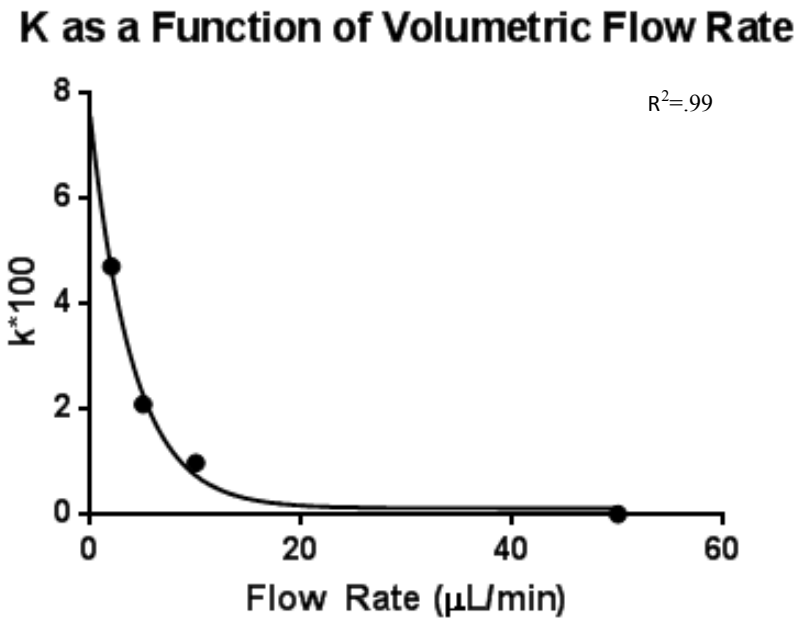


**Figure 9: k plotted as a function of the flow rate of the system.**

In Full:

$$AII = A_0 * (1 - \exp(-(k_0 * \exp(k' * V)) * V)) + C \text{ (Equation 8)}$$

## 4.2 Dye Separation

We repeated the dye separation experiment as performed in the past.[13] In this particular case, however, we used fluorescein and rhodamine B, rather than fluorescein and Alexa 591.

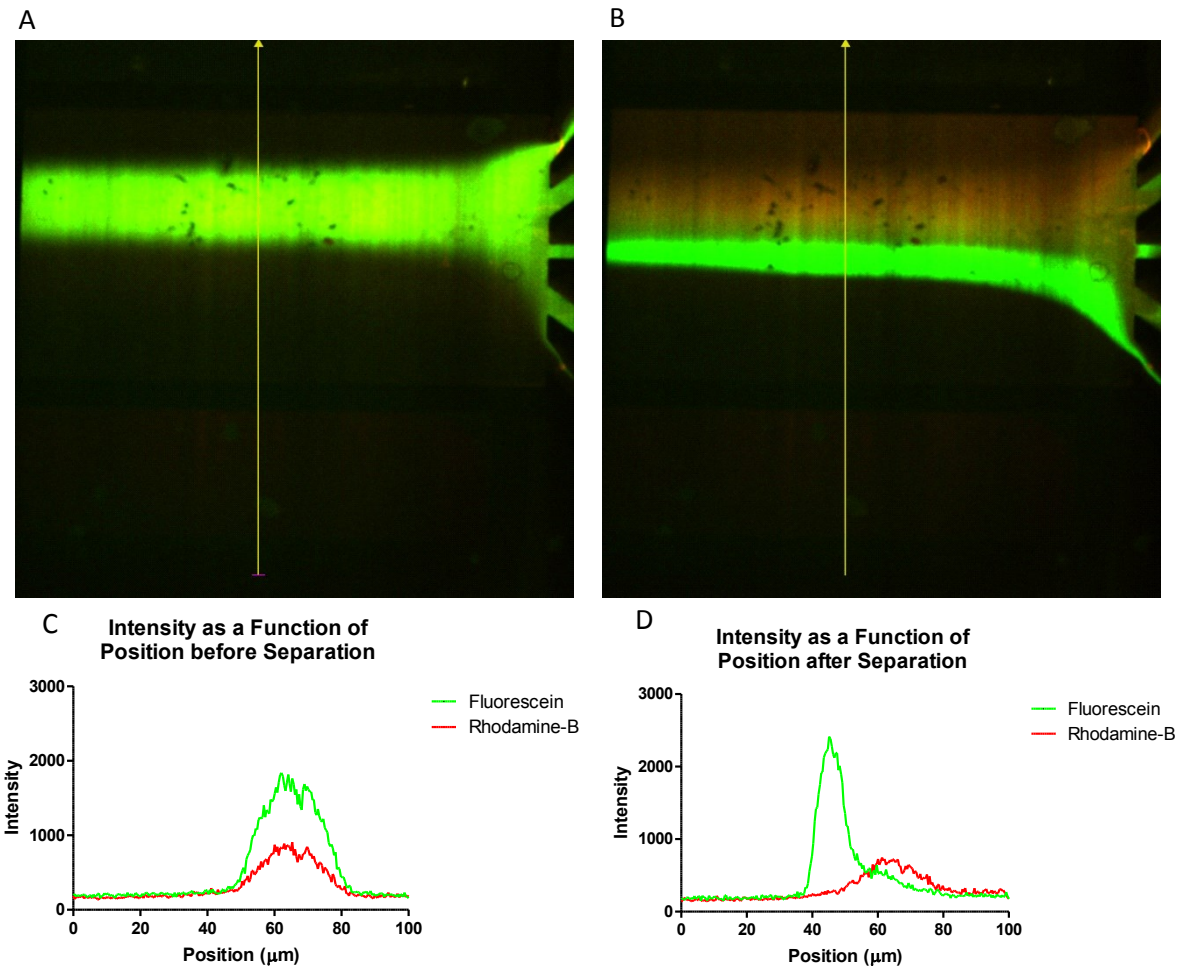


**Figure 10: A fluorescent image of the dye separation experiment with pre-sample mixing. Top left (10A) 5 µL/min, 0V. Top right (10B) 5 µL/min, 200 V. Bottom left (10C) concentration profile of figure 10A. Bottom right (10D) concentration profile of figure 10B.**

It is important to note the parameters of this experiment, we achieved separation at 200V and 5 µL/min. In past experiments, separation required 1800V in order to be effective at a flowrate of .5 µL/min.

## 4.3 Protein Focusing

We determined the next major step in the progression of our experiment to be the concentration of a protein in DI water. We achieved this utilizing the same setup as the concentration of dyes. In this case, we replaced the fluorescein with avidin-FITC.

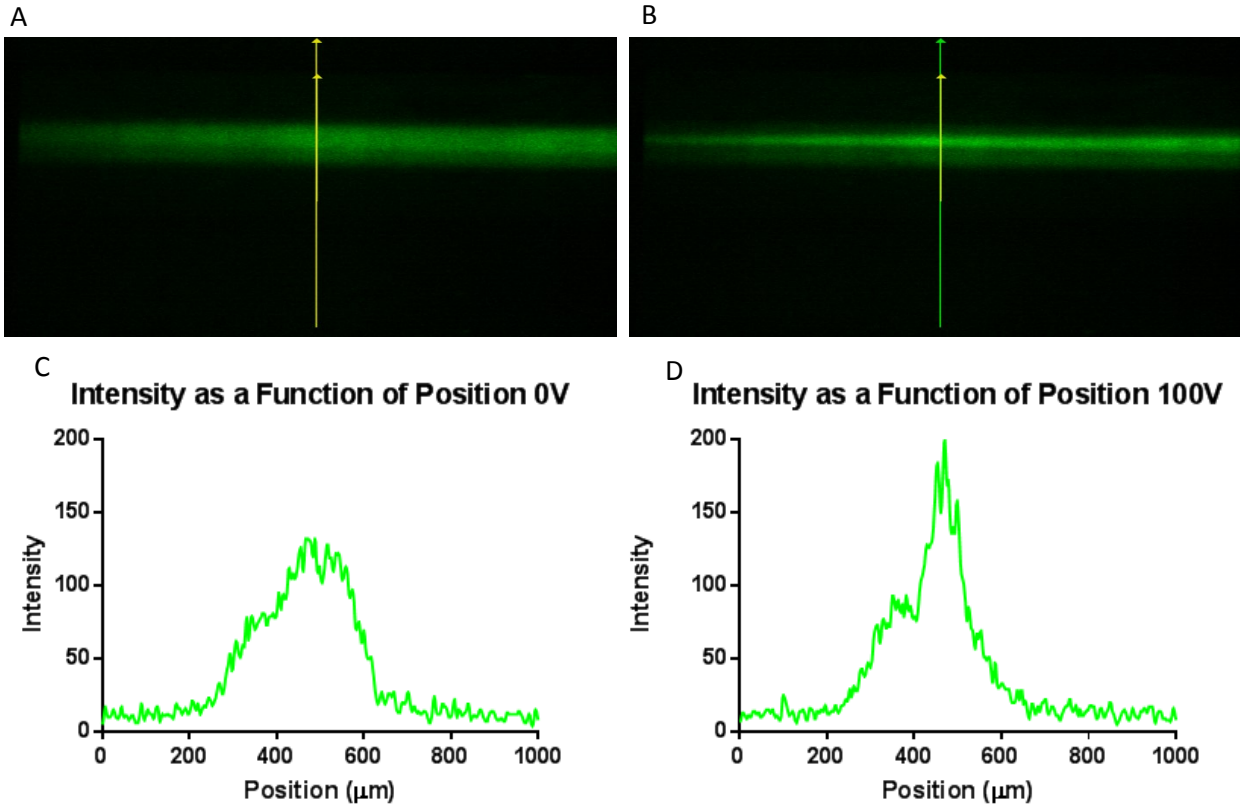


**Figure 11: A fluorescent image of the protein separation experiment without pre-sample mixing. Top left (11A) 5 µL/min 0V. Top right (11B) 5 µL/min 100 V. Bottom left (11C) concentration profile of figure 11A. Bottom right (11D) concentration profile of figure 11B.**

## 4.4 Protein Focusing in Serum

We decided it is important to explore the efficacy of our technology within a biologically relevant media. Thus, we repeated our avidin-FITC focusing experiment in human serum. All flowrates remained the same except for the flowrate of quinhydrone, which was increased to 15 µL/min.

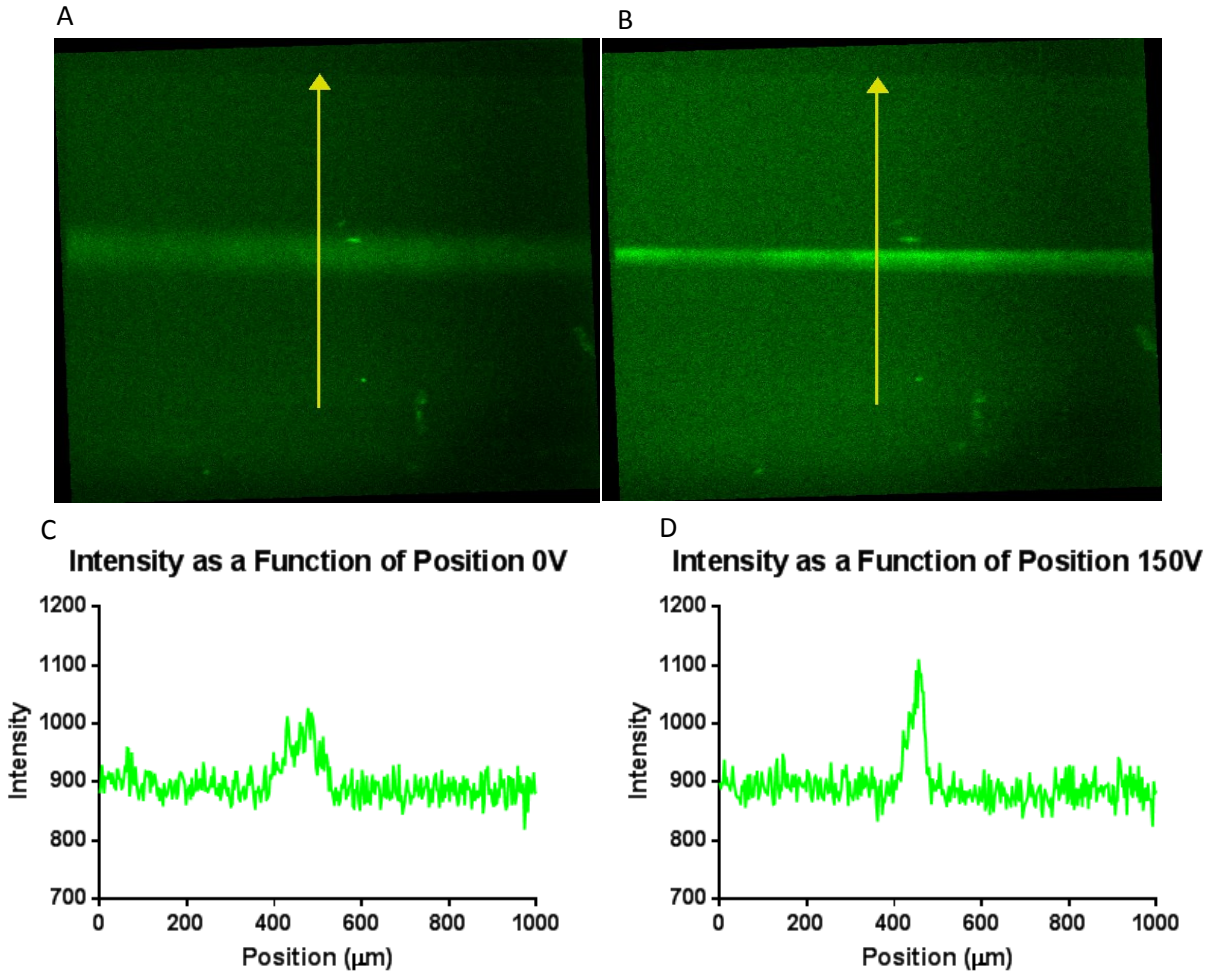


**Figure 12: A fluorescent image of the protein concentration experiment within human serum. Top left (12A) 5 µL/min, 0V. Top right (12B) 5 µL/min, 100 V. Bottom left (12C) concentration profile of figure 12A. Bottom right (12D) concentration profile of figure 12B.**

## 4.5 Critical Bubble Voltage

By altering the flowrate of quinhydrone, and slowly increasing the voltage applied across the channel, we were able to determine the critical bubble voltage at various flowrates.

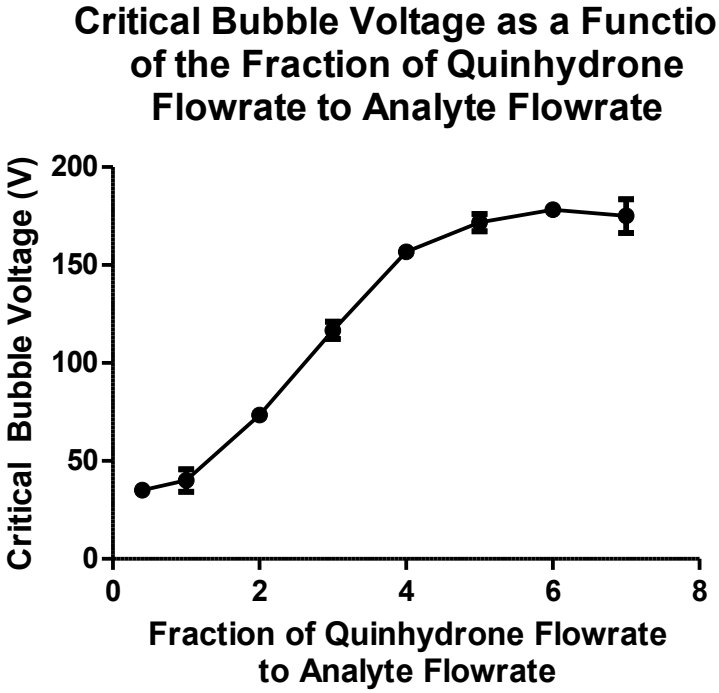


**Figure 13: Critical bubble voltage as a function of quinhydrone flowrate. Flowrate of TE, LE and Analyte: 5 µL/min.**

# Chapter 5

# Discussion

## 5.1 Dye Focusing

The change in methodology represents an improvement over our previous experimental setup. Removing the pre-mixing of the analyte and the TE makes our experiment easier to use, reducing the probability of human error. Further, considering the fact that pre-experimental steps are generally more time intensive than running microfluidic devices, the removal of the pre-mixing step will make future devices that utilize this technology more time efficient.

The development of a mathematical model improves our general understanding of the technology, making practical applications more attainable. Although our model is exclusively empirical, it is the first step in the direction of the development of a physical model, which would shine light on the significance of the constants in equation 8, and potentially further our understanding of the physical limitations of the device.

## 5.2 Dye Separation

The reduction in the required voltage to achieve separation represents an improvement in the efficiency of the device. This improved efficiency likely stems from improved fabrication techniques of both the carbon black application and the gallium injection. More specifically, less air bubbles get trapped between the electrode and the main channel when applying the carbon black doped PDMS, and less air bubbles get trapped when injecting the gallium. Both of these improvements in technique improve the electrical efficiency of the device. Finally, replacing

Alexa 591 with rhodamine B shows that our technology is capable of functioning with analytes that have a formal charge of 0.

From a qualitative standpoint, the separation was also quite effective. The majority of the area under the green curve does not interact with the area under the red curve in figure 12D.

## 5.3 Protein Focusing

Transitioning from dye to protein focusing presented a myriad of theoretical challenges. These challenges primarily arise from the fact that the electrophoretic mobility of a protein is heavily dependent on its conformation. Therefore, environmental factors including: heating, pH, and ionic strength can heavily influence the results of an experiment.

We plan to overcome the environmental dependency by moving into human serum (see below), and eventually into whole blood. Further, the challenge of denaturing due to Ohmic heating highlights the value of the carbon black membrane. By reducing the overall required voltage, the carbon black membrane mitigates the effects of Ohmic heating of the device.

## 5.4 Human Serum

Changing the media from DI water to human serum drastically increased the conductivity from electrode to electrode. As a result, bubbles began to form at a significantly lower threshold voltage due to the electrolysis of water. The lower bubble threshold not only reduces the efficacy of our technology, but also reduces the reliability as well. Not every device is exactly the same, and therefore the critical bubble voltage will change slightly from device to device. Theories for how we can combat the increased conductivity can be found in the future work section of this correspondence.

We partially combatted the formation of bubbles by increasing the flowrate of quinhydrone. This comes with the unfortunate side effect of pinching the analyte flow stream. This results in lower quality focusing, due to how tightly packed the input stream is upon entering the device in conjunction with physical packing limitations of dyes, proteins, and other analyes.

## 5.5 Critical Bubble Voltage

At a very low quinhydrone flowrate, the analyte takes up the majority of the channel, this area of high conductivity creates a very low critical bubble voltage. As the flowrate increases, the analyte takes up less of the main channel, and therefore, due to the overall lower conductivity through the channel, bubbles begin to form at a higher voltage threshold. As the analyte flow stream becomes more pinched, increasing the flow rate of the quinhydrone does little to improve the critical bubble voltage.

We found that we can achieve a voltage of 100V when the flow rate of quinhydrone is 3 times the flowrate of the analyte. Though our tests are possible at this voltage, and flow rate fraction, this level of pinching is not ideal. We will look to improve this in the future (see future work).

# Chapter 6

# Conclusion

Our long term goal is to develop a microfluidic device capable of monitoring the health of astronauts during long missions to deep space. We define the success of our device by its spatial efficiency, cost efficiency, weight efficiency, and its ease of use. In this correspondence, we improved on our previous method of utilizing ITP to develop a simultaneous western blot, and gel electrophoresis replacement. Our improvements include the development of a mathematical model to describe dye focusing, and overcoming challenges, and displaying efficacy in focusing protein focusing both in DI water, and human serum. Further, we have displayed the importance of high quality fabrication within these types of microfluidic devices, by drastically increasing the efficiency of the separation experiment. Finally, we have characterized the critical bubble voltage as a function of quinhydrone flowrate.

# Chapter 7

# Future Work

In the future, we plan on improving all experiments referenced in this correspondence. We plan to develop a physical model that aligns with our mathematical model, and explore the implications of the physical limits of the device with this model. This would bring us a step closer to developing practical devices with our technology.

We plan on repeating the dye focusing experiment with proteins, in order to ensure that the model we developed for dyes aligns with the model we developed for proteins. Further, we plan on expanding our work with proteins and human serum into the separation experiment in order to make our work more biologically relevant.

Due to the immense value gained simply by becoming more familiar with the fabrication techniques required to make this device, we plan on developing a less human based technique to apply the carbon black PDMS to the device, with the aim of improving overall reliability and efficiency.

In the future, we hope to find an electron acceptor that is more effective than quinhydrone. This would come with the benefit of being able to increase the width of the analyte flow stream without allowing for bubble formation, improving focusing effectiveness.

Further, we hope to repeat our work with proteins while using DNA as the analyte, and eventually move into using whole blood as the analyte.

In the very long term, we hope to determine how reusable our devices are, which could improve the devices overall spatial, weight, and cost efficiency. Finally, we hope to remove microscopy as a whole from our device, which would truly make our device portable and easy to use.

# References


1. Knapton, Sarah. "Elon Musk: We'll Create a City on Mars with a Million Inhabitants ." *The Telegraph*, Telegraph Media Group, 21 June 2017, www.telegraph.co.uk/science/2017/06/21/elon-musk-create-city-mars-million-inhabitants/.
2. Taylor, G. R., Konstantinova, I., Sonnenfeld, G. & Jennings, R. in 6, 1–32 (Elsevier, 1997).
3. Galts, Ciarán. A journey to Mars: *The Medical Challenges Associated with Deep Space Travel and Possible Solutions*. UBCMJ. 2017: 8.2 (38-39).
4. Dietlan, L. & Pestov I. Space Biology and Medicine. Volume IV, 1–464 (1996).
5. Kavermann, H., B. P. Burns, K. Angermuller, S. Odenbreit, W. Fischer, K. Melchers, and R. Haas. 2003. Identification and characterization of Helicobacter pylori genes essential for gastric colonization. J. Exp. Med. 197:813– 822.
6. Becker, H.; Locascio, L.E. Polymer microfluidic devices. Talanta 2002, 56, 267–287.
7. Bahga, Supreet S., Santiago, J. "Coupled Isotachophoretic Preconcentration and Electrophoretic Separation Using Bidirectional Isotachophoresis." *Analytical Chemistry*, vol. 83, no. 16, 2011, pp. 6154–6162., doi:10.1021/ac200268f.
8. Persat, A., Marshall, L. A., Santiago, J. G., Anal. Chem. 2009, 81, 9507–9511.
9. Rogacs, A., Qu, Y., Santiago, J. G., Anal. Chem. 2012, 84, 5858–5853.
10. Cui, H., Dutta, P., Ivory, C. F., Electrophoresis 2007, 28, 1138–1145.
11. Prest, J. E., Baldock, S. J., Fielden, P. R., Goddard, N. J. et al., J. Chromatogr. B Anal. Technol. Biomed. Life Sci. 2012, 903, 53–59.
12. Schwartz, O., Bercovici, M., Anal. Chem. 2014, 86, 10106–10113.
13. Fu, Xiaotong, et al. "Microfluidic Free-Flow Zone Electrophoresis and Isotachophoresis Using Carbon Black Nano-Composite PDMS Sidewall Membranes." *Electrophoresis*, vol. 38, no. 2, 2016, pp. 327–334., doi:10.1002/elps.201600104.
14. Yuvaraj, A.l., and D. Santhanaraj. "A Systematic Study on Electrolytic Production of Hydrogen Gas by Using Graphite as Electrode." *Materials Research*, vol. 17, no. 1, 2013, pp. 83–87., doi:10.1590/s1516-14392013005000153.
15. Gamboa-Valero, Nadia, et al. "Hydrogen Bonding Complexes in the Quinone-Hydroquinone System and the Transition to a Reversible Two-Electron Transfer Mechanism." *Electrochimica Acta*, vol. 188, 2016, pp. 602–610.
16. D. B. Weibel, W.R. DiLuzo and G.M. Whitesides, *Microfabrication meets microbiology*, Nature Rev. Microbiol. (2007), Vol. 5, No.3, pp. 208-218.

**Steven Doria**
3111 N. Charles St.
Baltimore, MD 21218
914-584-1835
sdoria1@jhu.edu

## Education

Johns Hopkins University
M.S.: Chemical and Biomolecular Engineering — Expected: May 2018
GPA: 3.90

B.S.: Chemical and Biomolecular Engineering — May 2017
Interfaces and Nanotechnology Concentration — ChemBe GPA: 3.92
Entrepreneurship and Management Minor — GPA: 3.62
Dean's List: Fall 2013, Spring 2014, Fall 2014, Fall 2015, Fall 2016, Spring 2017

## Awards

**Deloitte Case Competition – First Place Winner** — Spring 2018
- Received a case study with 3 days preparation
- Prepared and presented a multi-faceted solution

**Deloitte Case Competition – Second Place Winner** — Spring 2016
- Received a case study with 3 days preparation
- Prepared and presented a multi-faceted solution

**Elnora Streb Muly Award** — Spring 2015
- Awarded for excellence in independent chemical engineering research on problems identified by engineers working in industry

## Publications

**Lab on a Chip, 17, 2015: Microfluidic Pumping, Routing and Metering by Contactless Metal-Based Electro-Osmosis** — Summer 2015

## Employment

**CPA Global** — Spring 2018 – Present
*Remote Patent Analyst*
- Independently researched and analyzed prior patents similar to a given pending patent
- Delivered reports on technical aspects of patents

**Johns Hopkins University** — Fall 2013 – Present
*Microfluidics Research Assistant – Gagnon Lab*
- Developed, tested, troubleshot, and analyzed various microfluidic devices
- Collected and analyzed data on projects using aforementioned devices
- Microfabrication of PDMS based devices in a clean room environment
- Fluorescent microscopy of microfluidic devices

## Italian Club

- Treasurer — Spring 2016 – Fall 2016
- Events Coordinator — Spring 2015 – Fall 2015

## Interests and Special Skills

- Computer Programming: Java, Python, Matlab, and Maple
- Lab Skills: Microfluidic troubleshooting, fluorescent microscopy, and microfabrication